ARTICLES

Ultrafast FRET in a Room Temperature Ionic Liquid Microemulsion: A Femtosecond Excitation Wavelength Dependence Study†

Aniruddha Adhikari, Dibyendu Kumar Das, Dibyendu Kumar Sasmal, and Kankan Bhattacharyya*

Department of Physical Chemistry, Indian Association for the Cultivation of Science, Jadavpur, Kolkata 700 032, India

Received: October 4, 2008; Revised Manuscript Received: December 2, 2008

Fluorescence resonance energy transfer (FRET) from coumarin 480 (C480) to rhodamine 6G (R6G) is studied in a room temperature ionic liquid (RTIL) microemulsion by picosecond and femtosecond emission spectroscopy. The microemulsion is comprised of the RTIL 1-pentyl-3-methylimidazolium tetraflouroborate, [pmim][BF_4], in TX-100/ benzene. We have studied the microemulsion with and without water. The time constants of FRET were obtained from the risetime of the acceptor (R6G) emission. In the RTIL microemulsion, FRET occurs on multiple time scales: 1, 250, and 3900 ps. In water containing RTIL microemulsion, the rise components are 1.5, 250, and 3900 ps. The 1 and 1.5 ps components are assigned to FRET at a close contact of donor and acceptor ($R_{DA} \approx 12$ Å). This occurs within the highly polar (RTIL/water) pool of the microemulsion. With increase in the excitation wavelength (λ_{ex}) from 375 to 435 nm, the relative contribution of the ultrafast component of FRET ($\sim$1 ps) increases from 4% to 100% in the RTIL microemulsion and 12% to 100% in the water containing RTIL microemulsion. It is suggested that at $\lambda_{ex} = 435$ nm, mainly the highly polar RTIL pool is probed where FRET is very fast due to the close proximity of the donor and the acceptor. The very long 3900 ps ($R_{DA} \approx 45$ Å) component may arise from FRET from a donor in the outer periphery of the microemulsion to an acceptor in the polar RTIL pool. The 250 ps component ($R_{DA} \approx 29$ Å) is assigned to FRET from a donor inside the surfactant chains.

1. Introduction

Room temperature ionic liquids (RTILs) have attracted a lot of recent attention as environmentally benign ("green") solvents, for their wide temperature range and as catalysts in many organic reactions.[1−7] More recently, many groups have reported formation of micelles[8,9] and reverse micelles[10,11] involving RTIL-s. Eastoe et al.[10a] and Gao et al.[10b] reported formation of microemulsion with a pool of the RTIL, [bmim][BF_4] inside a reverse micelle containing the surfactant, triton-X-100 (TX-100) in a hydrocarbon. From SANS studies, Eastoe et al. concluded that the ionic liquid pool is ellipsoidal in shape with a semiminor radius of 2.4 nm and a length of 11 nm for an equimolar ratio of ([bmim][BF_4]) and the surfactant (TX-100).[10a] Gao et al. reported that as much as 6 wt % water may be encapsulated in the polar nanodomain of such a microemulsion.[10b] We have previously studied a similar system employing the ionic liquid 1-pentyl-3-methylimidazolium tetraflouroborate, [pmim][BF_4], in TX-100/ benzene microemulsion.[11] In such a heterogeneous environment, the polarity varies from a hydrocarbon-like environment within the alkyl chains of the surfactants at the interface to a polar environment inside the ionic liquid pool.

In our previous work, we had studied solvation dynamics in different regions of an ionic liquid microemulsion[11a] and a RTIL mixed micelle.[11b] We had probed different regions of the ionic liquid microemulsion by variation of excitation wavelength (λ_{ex}). This is based on the simple fact that the absorption maximum of the solvatochromic probe varies with polarity: a short λ_{ex} selects the probe molecules in a relatively nonpolar environment (near the surfactant chains at the interface), while a long λ_{ex} excites the molecules in a polar region, e.g., core of the ionic liquid pool. This is based on the so-called Red Edge Excitation Shift (REES).[12,13] The λ_{ex} dependence of solvation dynamics has also been used to reveal dynamic heterogeneity in a neat RTIL.[2a,11a] In the case of a RTIL microemulsion, we observed that with increase in λ_{ex} anisotropy decay becomes slower while solvation dynamics becomes faster.[11a] This was rationalized as follows. The viscosity of an ionic liquid is much higher than that of an alkane.[1] Hence, the viscosity at the core of the RTIL microemulsion is much higher than that at the interface. Thus the core is more polar and more viscous than the alkyl chain region of the surfactants (interface). A long λ_{ex} probes the highly viscous core of the solvent pool and hence shows slow anisotropy decay. In the case of solvation dynamics, movement of the polar species (head groups and ions) is restricted at the interface region but is more free at the core of the pool. This makes solvation faster at long λ_{ex}.[11]

In the present work, we investigate fluorescence resonance energy transfer (FRET) in different regions of a RTIL microemulsion containing, [pmim][BF_4] (Scheme 1A) and the surfactant TX-100 in benzene (Scheme 1B). We have chosen an ionic dye (rhodamine 6G, R6G, Scheme 1C) as the acceptor.

† Part of the "George C. Schatz Festschrift".

* Corresponding author. E-mail: pckb@iacs.res.in.

10.1021/jp808777w CCC: $40.75
Published on Web 01/07/2009

SCHEME 1: Structure of (A) [pmim][BF_4], (B) [pmim][BF_4]/TX-100/Benzene, (C) R6G, and (D) C480

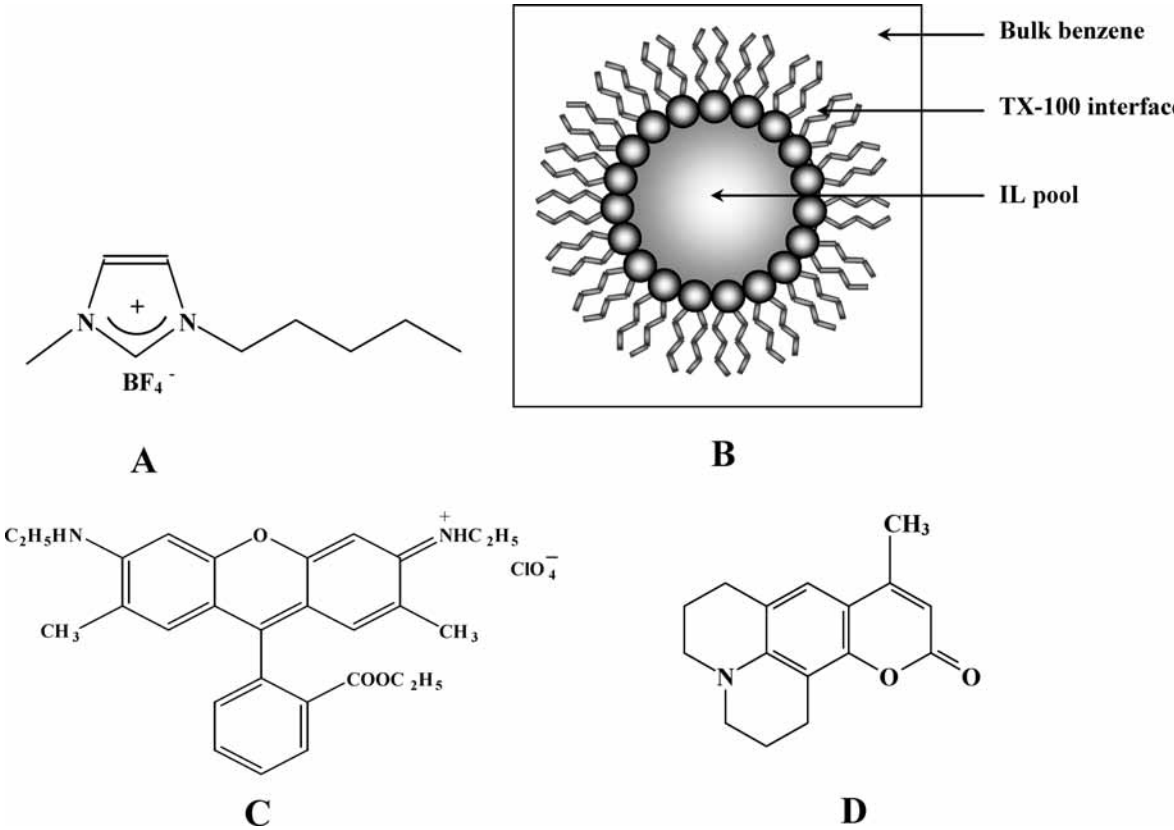

The acceptor being an ion preferentially stays in the core of the ionic liquid pool. The donor is a neutral molecule (coumarin 480, C480, Scheme 1D) and hence is distributed over different regions of the entire microemulsion. This results in a wide distribution of the donor−acceptor distances (R_{DA}). According to Forster theory, the rate of FRET is inversely proportional to the sixth power of the distance between the donor and the acceptor. In this work, we have tried to study FRET from the donors residing in different regions. This was achieved through variation of λ_{ex}. At a short λ_{ex}, a donor (C480) molecule in a relatively nonpolar region near the surfactant chains is excited while at a long λ_{ex}, a donor in the polar region (core of the ionic liquid pool) is excited. In the first case (short λ_{ex}) R_{DA} is large, while in the second case R_{DA} is small. This is expected to affect the rate of FRET. We have previously employed this technique to study FRET in a reverse micelle,[14a] a triblock copolymer micelle and gel,[14b] and a bile salt aggregate.[14c] In the present work, we examine how λ_{ex} variation affects FRET in a RTIL microemulsion.

2. Experimental Section

Laser grade coumarin 480 (C480, Exciton, Scheme 1D) and rhodamine 6G (R6G, Exciton, Scheme 1C) were used as received. The concentrations of the donor (C480) and acceptor (R6G) were kept fixed at 40 and 80 μM, respectively.

Sodium tetrafluoroborate (98%, Aldrich), 1-methylimidazole (99%, Aldrich), and 1-bromopentane (99%, Aldrich) were used for the synthesis of the room temperature ionic liquid. Acetonitrile (Merck) was distilled over P_2O_5 and dichloromethane (Merck) was used as received. Diethyl ether (Merck) was distilled over KOH. TX-100 (Nacalai Tesque) was vaccuum-dried for about 2 h before the experiments while benzene (UV grade, Spectrochem) was dried over sodium.

The RTIL, [pmim][Br] was prepared from 1-methylimidazole and 1-bromopentane following a sonochemical route.[15a] Pure [pmim][BF_4] (Scheme 1B) was obtained through the metathesis of [pmim][Br] with $NaBF_4$ in dry acetonitrile under argon atmosphere at room temperature.[15b,c] For purification, the crude [pmim][BF_4] was diluted with dicholoromethane and filtered a couple of times through a silica gel column. The filtrate was treated with activated charcoal in an inert atmosphere for 48 h to remove any possible trace of color. After removal of dicholoromethane in a rotary evaporator, [pmim][BF_4] was repeatedly washed with dry diethyl ether to yield the RTIL in the form of a colorless, viscous liquid.

The steady state absorption and emission spectra were recorded in a Shimadzu UV-2401 spectrophotometer and a Spex FluoroMax-3 spectrofluorimeter, respectively.

In our femtosecond upconversion setup (FOG 100, CDP) the sample was excited at 375, 405, and 435 nm, respectively, using the second harmonic of a mode-locked Ti-sapphire laser (Tsunami, Spectra Physics), pumped by a 5 W Millennia (Spectra Physics). To generate second harmonic we used a nonlinear crystal (1 mm BBO, $\theta = 25°$, $\phi = 90°$). The fluorescence emitted from the sample was upconverted in a nonlinear crystal (0.5 mm BBO, $\theta = 38°$, $\phi = 90°$) by using the fundamental beam as a gate pulse. The upconverted light is dispersed in a monochromator and detected by using photon counting electronics. A cross-correlation function obtained with use of the Raman scattering from ethanol displayed a full width at half-maximum (fwhm) of 350 fs. The femtosecond fluorescence decays were fitted by using a Gaussian shape for the exciting pulse.

To fit the femtosecond data one needs to know the long decay components. They were detected by using a picosecond setup. For this purpose, the samples were excited at 375, 405, and

435 nm with picosecond diode lasers (IBH nanoleds) in an IBH Fluorocube apparatus. The emission was collected at a magic angle polarization with a Hamamatsu MCP photomultiplier (5000U-09). The time correlated single photon counting (TC-SPC) setup consists of an Ortec 9327 CFD and a Tennelec TC 863 TAC. The data are collected with a PCA3 card (Oxford) as a multichannel analyzer. The typical fwhm of the system response with use of a liquid scatterer is about 90 ps. The picosecond fluorescence decays were deconvoluted by using IBH DAS6 software. All experiments were done at room temperature (293 K).

To fit the femtosecond transients, we first determined the long picosecond components by deconvolution of the picosecond decays. Then the long picosecond components were kept fixed to fit the femtosecond data.

The rate of FRET (k_{FRET}) was calculated by using the Förster theory as,[16]

$$k_{FRET} = \frac{1}{\tau^{A}_{rise}} = \frac{1}{\tau^{0}_{D}}\left(\frac{R_0}{R_{DA}}\right)^6 \quad (1)$$

where, τ^0_D is the lifetime of the donor in the absence of acceptor and τ^A_{rise}, is the risetime of acceptor emission in the presence of donor. At a donor−acceptor distance $R_{DA} = R_0$, the efficiency of energy transfer is 50% and $k_{FRET} = (1/\tau^0_D)$. To calculate the Förster distance R_0 (in Å) we used,[16]

$$R_0 = 0.211[\kappa^2 n^{-4} Q_D J(\lambda)]^{1/6} \quad (2)$$

where n is the refractive index of the medium (~1.4 for macromolecules in water),[16] Q_D is the quantum yield of the donor in the absence of acceptor, κ^2 is the orientation factor, and $J(\lambda)$ is the spectral overlap between the donor emission and the acceptor absorption. $J(\lambda)$ is related to the normalized fluorescence intensity (F_D) of the donor in the absence of the acceptor and the extinction coefficient of the acceptor (ε_A) as,[16]

$$J(\lambda) = \frac{\int_0^\infty F_D(\lambda)\varepsilon_A(\lambda)\lambda^4\, d\lambda}{\int_0^\infty F_D(\lambda)\, d\lambda} \quad (3)$$

The value of κ^2 may vary from 0 (mutually perpendicular transition dipoles) to 4 (collinear dipoles). For $\kappa^2 = 0$, FRET is forbidden and no ultrafast component of FRET would be observed. The ultrafast FRET detected in this work obviously indicates a large value of κ^2. One can estimate the upper (κ^2_{max}) and lower (κ^2_{min}) limit of κ^2 from the steady state fluorescence anisotropy and the initial value of anisotropy (r_0) obtained in the time-resolved anisotropy measurement as,[16]

$$\kappa^2_{min} = \frac{2}{3}\left[1 - \frac{(d^x_D + d^x_A)}{2}\right] \quad (4)$$

$$\kappa^2_{max} = \frac{2}{3}(1 + d^x_D + d^x_A + 3d^x_D d^x_A) \quad (5)$$

where, d^x_i denotes the ratio of the square root of the steady state fluorescence anisotropy (r^{SS}_i) and the initial value of anisotropy (r^0_i) in the anisotropy decay of the ith species (donor or acceptor). The distance calculated by using the Förster model is found to vary by only about ≤20% in the range of values of κ^2. We therefore used $\kappa^2 = {}^2/_3$ (random orientation) for the calculation of R_0.

3. Results

3.1. Steady State Study of FRET in [pmim][BF4]/TX-100/

TABLE 1: Energy Transfer Parameters for the C480−R6G Pair in Different Systems

system	λ_{ex} (nm)	λ_{em} (C480) (nm)	$J(\lambda)^a$ (M^{-1} cm^{-1} nm^4)	$R_0{}^a$ (Å)	$\varepsilon_s{}^a$
RTIL microemulsion	375	451	0.80×10^{15}	44	0.35
	405	453	0.85×10^{15}	45	0.33
	435	457	1.10×10^{15}	47	0.36
RTIL microemulsion with 5 wt % water	375	460	1.05×10^{15}	46	0.43
	405	462	1.20×10^{15}	47	0.43
	435	466	1.40×10^{15}	49	0.45

[a] ±10%.

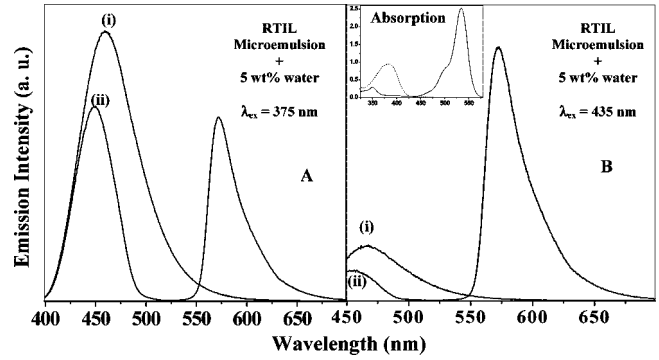

Figure 1. Emission spectrum of 40 μM C480 in [pmim][BF_4]/TX-100/benzene/water microemulsion λ_{ex} at (A, B) 375 and 435 nm in the absence (i) and in the presence (ii) of 80 μM R6G. The inset shows the absorption spectra of C480 (---) and R6G (—).

Benzene Microemulsions: λ_{ex} Dependence. In the RTIL microemulsion, the emission maximum of the acceptor (R6G) is found to be independent of λ_{ex}. This indicates that the acceptor R6G resides in a more or less uniform environment. Because of its positive charge, R6G seems to reside within the polar ionic pool of the RTIL microemulsion.

The donor is distributed in both polar (RTIL pool) and nonpolar regions of the microemulsion. In the RTIL microemulsion without water, with increase in λ_{ex}, the emission spectrum of the donor (C480) exhibits a red shift and the emission maximum exhibits a 6 nm REES from 451 nm at λ_{ex} = 375 nm to 457 at λ_{ex} = 435 nm. The emission maxima of C480 in the RTIL microemulsion are close to the reported[17] emission maximum of C480 in acetonitrile (450 nm). Hence, the microenvironment of C480 in the RTIL microemulsion resembles acetonitrile in polarity. The REES suggests that the donor (C480) is distributed over different regions of varying polarity within the microemulsion.

In the presence of 5 wt % water, the emission maximum of C480 in RTIL microemulsion exhibits a ~9 nm red shift compared to that without water at all λ_{ex}. This suggests that the water containing RTIL microemulsion is more polar than that without water. Note the emission maxima in water containing microemulsion are red-shifted from those without water. However, REES (which measures differences in polarity) is similar in both cases (with and without water, Table 1).

In the RTIL microemulsion, emission intensity of the donor (C480) decreases by 30−40% on addition of the acceptor (R6G) (Figure 1). This is ascribed to FRET from C480 to R6G. The steady state efficiency (ε_s) of FRET is calculated by using the following relationship, $\varepsilon_s = 1 - (I_{DA}/I_D)$, where I_{DA} and I_D denote steady state emission intensity of the donor in the presence and absence of the acceptor, respectively.[16] The efficiency of FRET (ε_s) at different excitation wavelengths is summarized in Table 1.

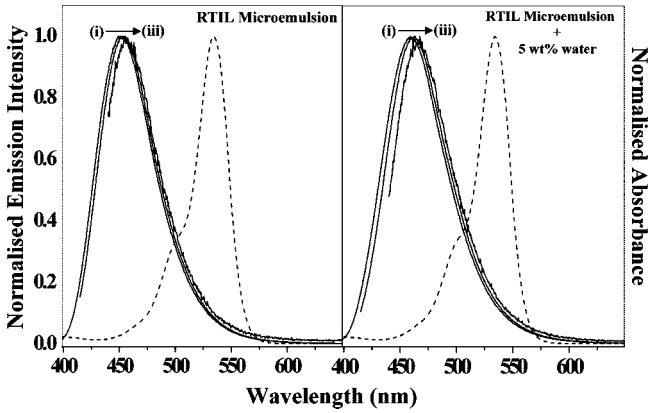

Figure 2. Overlap spectra between donor (C480) emission (—) in (A, left) [pmim][BF_4]/TX-100/benzene and (B, right) [pmim][BF_4]/TX-100/benzene/water microemulsion with acceptor (R6G) absorption (---) at λ_{ex} (i−iii) 375, 405, and 435 nm.

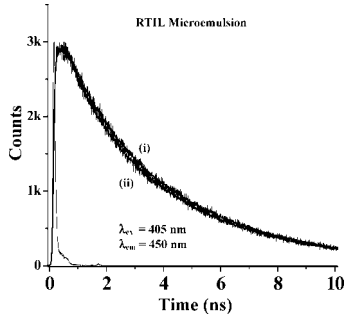

Figure 3. Picosecond decays (λ_{em} = 450 nm) of the donor (C480, 40 μM) with (i) 0 μM and (ii) 80 μM R6G in [pmim][BF_4]/TX-100/benzene/water microemulsion at λ_{ex} = 405 nm.

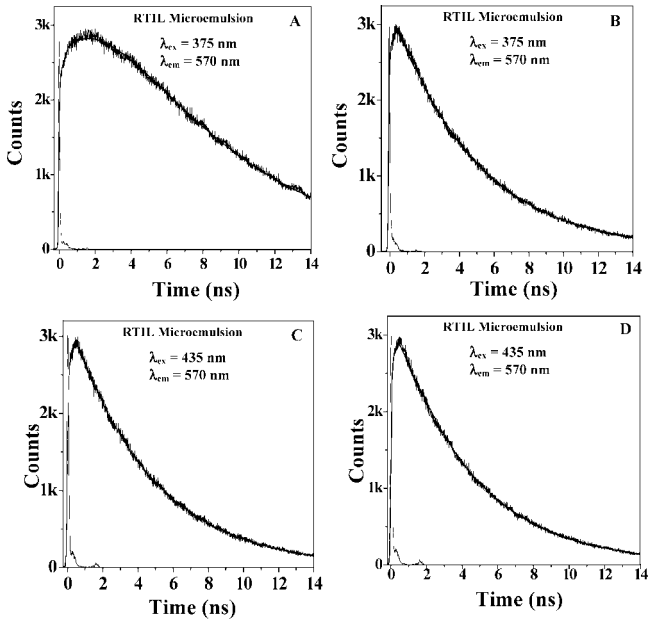

Figure 4. Picosecond transients (λ_{em} = 570 nm) of the acceptor (R6G, 80 μM) in [pmim][BF_4]/TX-100/benzene microemulsion with (A) 40 μM C480, (B) 0 μM C480, (C) 40 μM C480, and (D) 0 μM C480; at λ_{ex} = 375 nm (A, B) and λ_{ex} = 435 nm (C, D).

Figure 2 shows the overlap between the absorption spectrum of the acceptor (R6G) with the emission spectrum of the donor (C480) in the RTIL microemulsion and water containing RTIL microemulsion at different excitation wavelengths (λ_{ex}). The values of the spectral overlap integral, $J(\lambda)$, between the emission spectrum of the donor (C480) and absorption spectrum

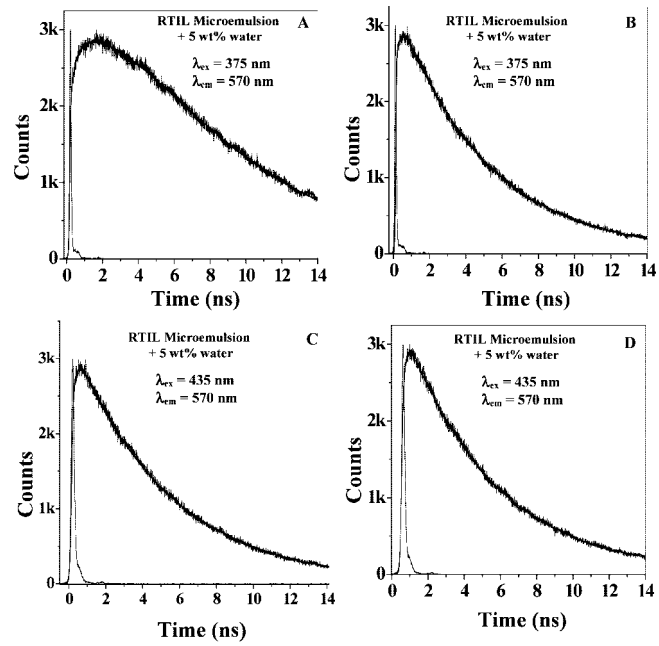

Figure 5. Picosecond transients (λ_{em} = 570 nm) of the acceptor (R6G, 80 μM) in [pmim][BF_4]/TX-100/benzene/water microemulsion with (A) 40 μM C480, (B) 0 μM C480, (C) 40 μM C480, and (D) 0 μM C480; at λ_{ex} = 375 nm (A, B) and λ_{ex} = 435 nm (C, D).

TABLE 2: Picosecond Decay Parameters of R6G (80 μM, λ_{em} = 570 nm) in the Presence of C480 (40 μM) at Different λ_{ex} Values

system	λ_{ex} (nm)	$\tau_1{}^a$ ($a_1{}^b$) (ps)	$\tau_2{}^a$ ($a_2{}^b$) (ps)	$\tau_3{}^a$ ($a_3{}^b$) (ps)
RTIL microemulsion	375	250 (−0.18)	3900 (−4.44)	5300 (5.62)
	405	250 (−0.13)	3900 (−3.40)	5300 (4.53)
	435			4600 (1.00)
RTIL microemulsion + 5 wt % water	375	250 (−0.24)	3900 (−3.57)	5600 (4.81)
	405	250 (−0.17)	3900 (−2.88)	5600 (4.05)
	435			5200 (1.00)

[a] ±10%. [b] a_i denote the amplitudes of a decay, $\sum a_i \exp(-t/\tau_i)$.

of the acceptor (R6G) at different excitation wavelengths are given in Table 1. Because of the red shift of the donor emission, the magnitude of the spectral overlap, $J(\lambda)$, increases about 40% as λ_{ex} increases from 375 to 435 nm (Table 1). However, the steady state efficiency of FRET does not increase appreciably with an increase in λ_{ex}. This may be due to the fact that in only a few microemulsions both the donor and the acceptor are present. In most cases, a microemulsion contains only the donor and these non-FRET donors dominate the fluorescence intensity. In keeping with this observation, Förster distance (R_0) values, calculated from steady state spectra,[16] do not change significantly with λ_{ex} in the RTIL microemulsion (Table 1).

We will discuss later that the donor−acceptor distances may be most reliably calculated from the rise of the acceptor fluorescence using eq 1. When it is done that way a marked λ_{ex} dependence of FRET is observed.

3.2. Time-Resolved Studies of FRET from C480 to R6G in RTIL Microemulsions. ***3.2.1. Picosecond Studies.*** In the [pmim][BF_4]/TX-100/benzene microemulsions (both with and without water), the donor lifetime recorded in a picosecond setup remains almost unchanged on addition of acceptor (R6G) (Figure 3). It seems that in both cases the donor emission is dominated by the unquenched non-FRET donors and hence no shortening of the donor lifetime is detected in a picosecond setup. Since the picosecond decay of the donor does not

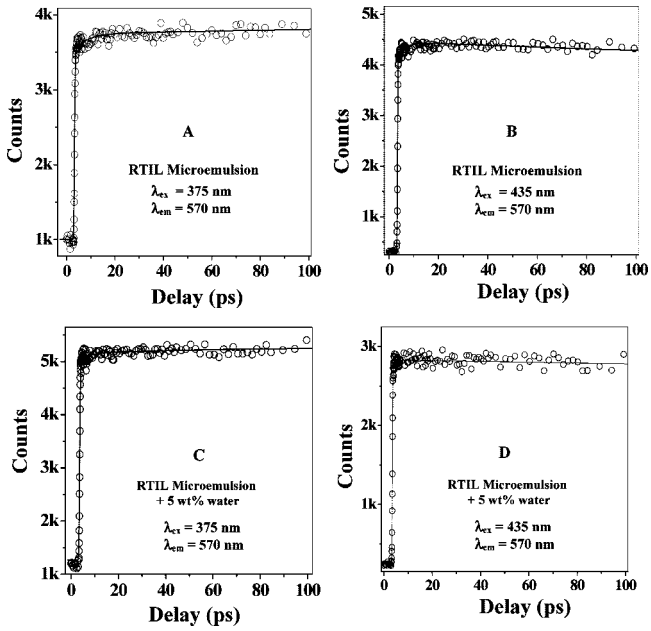

Figure 6. Femtosecond transients (λ_{em} = 570 nm) of the acceptor (R6G, 80 μM) in the presence of 40 μM C480 (donor), in [pmim][BF_4]/TX-100/benzene microemulsion (A, B) and [pmim][BF_4]/TX-100/benzene/water microemulsion (C, D); at λ_{ex} = 375 nm (A, C) and λ_{ex} = 435 nm (B, D).

TABLE 3: Femtosecond Decay Parameters of R6G (80 μM, λ_{em} = 570 nm) in the Absence of C480 at Different λ_{ex} Values

system	λ_{ex} (nm)	$\tau_1{}^a$ ($a_1{}^b$) (ps)	$\tau_2{}^a$ ($a_2{}^b$) (ps)
RTIL microemulsion	375	100 (0.04)	4900 (0.96)
	405	100 (0.15)	5000 (0.85)
	435	100 (0.20)	4600 (0.80)
RTIL microemulsion + 5 wt % water	375	100 (0.01)	5000 (0.99)
	405	100 (0.05)	4900 (0.95)
	435	100 (0.12)	4800 (0.88)

[a] ±10%. [b] a_i denote the amplitudes of a decay, $\sum a_i \exp(-t/\tau_i)$.

correctly describe the ultrafast FRET, we monitored FRET from the rise of the acceptor emission. In this section we report the long component of FRET detected in a picosecond setup. In the next section, we will discuss detection of the ultrafast component of FRET using a femtosecond setup.

Figures 4 and 5 show picosecond fluorescence transients of the acceptor (R6G) at 570 nm in the [pmim][BF_4]/TX-100/benzene and [pmim][BF_4]/TX-100/benzene/water microemulsions in the absence and presence of the donor (C480) at different λ_{ex} values. In this work, we have studied the fluorescence transient of the acceptor (R6G) at an emission wavelength 570 nm. At this wavelength, the contribution of the quenched emission of the donor is negligible. In the absence of the donor

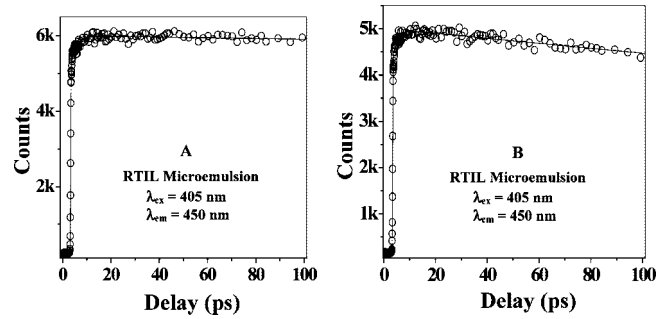

Figure 7. Femtosecond transients (λ_{em} = 450 nm) of 40 μM C480 (donor) in [pmim][BF_4]/TX-100/benzene microemulsion (A) in the absence and (B) in the presence of 80 μM R6G (λ_{ex} = 405 nm).

TABLE 5: Donor−Acceptor Distances in the RTIL Microemulsion, [pmim][BF_4]/TX-100/Benzene Calculated from Rise of Acceptor Emission

system	λ_{ex} (nm)	τ_{fret} (ps)	$R_{DA}{}^a$ (Å)
0 wt % water	375	1, 250, 3900	11, 28, 44
	405	1, 250, 3900	11, 28, 45
	435	1	12
5 wt % water	375	1.5, 250, 3900	13, 30, 46
	405	1.5, 250, 3900	13, 30, 47
	435	1.5	13

[a] ±10% with $\tau_{fret} = \tau_{rise}$ [since, τ_D°(~3.9 ns) < τ_A(~5 ns)].

(C480), at all λ_{ex}, the acceptor (R6G) exhibits a single exponential decay (~4600−5000 ps) with no rise component in both systems. However, in the presence of the donor (C480), picosecond transients of the acceptor (R6G) at 570 nm show distinct rise components at λ_{ex} = 375 and 405 nm in RTIL microemulsion. The observed rise components are ascribed to FRET from C480 to R6G. For λ_{ex} = 375 and 405 nm, the rise components (i.e., FRET) are 250 and 3900 ps in the RTIL microemulsion (Figure 4 and Table 2).

In the water containing RTIL microemulsion, picosecond transients of the acceptor (R6G) also exhibit similar rise (i.e., FRET) components for λ_{ex} = 375 and 405 nm.

For both [pmim][BF_4]/TX-100/benzene and [pmim][BF_4]/TX-100/benzene/water microemulsions, for a long wavelength of excitation (λ_{ex} = 435 nm) we did not detect any rise in the acceptor emission in our picosecond setup (Figures 4 and 5, Table 2). This indicates that for λ_{ex} = 435 nm, FRET is too fast to be detected in our picosecond setup (IRF ≈ 90 ps).

3.2.2. Femtosecond Study of the Ultrafast Component of FRET from the Rise of the Acceptor Fluorescence. The ultrafast components of FRET were detected by using a femtosecond setup. Figure 6 shows the ultrafast rise of the acceptor (R6G) at an emission wavelength of 570 nm in the [pmim][BF_4]/TX-100/benzene microemulsions at different excitation wavelengths. For all λ_{ex}, we detected an ultrafast rise

TABLE 4: Femtosecond Decay Parameters of R6G (80 μM, λ_{em} = 570 nm) in the Presence of C480 (40 μM) at Different λ_{ex} Values

system	λ_{ex} (nm)	$\tau_1{}^a$ ($a_1{}^b$) (ps)	$\tau_2{}^a$ ($a_2{}^b$) (ps)	$\tau_3{}^a$ ($a_3{}^b$) (ps)	$\tau_4{}^a$ ($a_4{}^b$) (ps)
RTIL microemulsion	375	1 (−0.15, 4%)	250 (−0.25, 6%)	3900 (−3.5, 90%)	5300 (4.9)
	405	1 (−0.10, 12%)	250 (−0.06, 6%)	3900 (−0.72, 82%)	5300 (1.88)
	435	1 (−0.11, 100%)			4600 (1.11)
RTIL microemulsion + 5 wt % water	375	1.5 (−0.08,12%)	250 (−0.07, 10%)	3900 (−0.57, 78%)	5600 (1.72)
	405	1.5 (−0.15, 21%)	250 (−0.10, 14%)	3900 (−0.46,65%)	5600 (1.71)
	435	1.5 (−0.03, 100%)			5200 (1.03)

[a] ±10%. [b] a_i denote the amplitudes of a decay, $\sum a_i \exp(-t/\tau_i)$.

component for both the RTIL microemulsion with rise times ~1 ps in the absence of water and 1.5 ps in the presence of water, in addition to those detected with the picosecond setup. Note, in the absence of the donor, no rise component is observed in the acceptor emission (Table 3). As shown in Table 4, the relative contribution of the ultrafast component increases markedly with increase in λ_{ex}. In the following section, we will discuss the origin of the ultrafast component of FRET and explain the λ_{ex} dependence.

Figure 7 shows fluorescence decays of donor lifetime in RTIL microemulsion in the femtosecond time scale ($\lambda_{em} = 450$ nm). It is readily seen that addition of the acceptor causes the appearance of an ultrashort component of the decay of the donor fluorescence. The appearance of the ultrashort decay of the donor emission and a rise in acceptor's emission unequivocally proves the occurrence of ultrafast FRET from the donor (C480) to an acceptor (R6G) in the RTIL microemulsion.

4. Discussion

This work demonstrates that femtosecond spectroscopy is a very sensitive tool to detect ultrafast FRET in an RTIL microemulsion. We have noted already that the steady state spectra is dominated by non-FRET donors and does not reveal the time constant of FRET. From the rise of the acceptor emission we detected three different time constants of FRET in the RTIL microemulsion: 1, 250, and 3900 ps, in the absence of water and 1.5, 250, and 3900 ps in the presence of water.

From the time constant of FRET, the donor−acceptor distances, R_{DA}, were calculated with eq 1. This corresponds to three distinct D−A distances of ~12 ± 1, 29 ± 1, and 45 ± 2 Å. These distances are smaller than the size of the microemulsion. According to our previous dynamic light scattering (DLS) studies,[11a] the radius of the RTIL microemulsion is ~160 Å in the absence of water and ~43 Å in the presence of water (5 wt %). $R_{DA} = 12$ Å is very close to the sum of radii of the donor and the acceptor molecule. Since the ionic acceptor resides in the ionic liquid pool, the 12 Å D−A distance corresponds to a donor and an acceptor residing at close proximity in the RTIL pool of the microemulsion. The very large D−A distance of 45 ± 2 Å may arise from a donor residing in the outer periphery of the microemulsion to an acceptor inside the polar RTIL pool. $R_{DA} = 45$ Å may also involve diffusion of a donor from bulk benzene into the microemulsion. The 250 ps component ($R_{DA} \approx 29$ Å) corresponds to an intermediate situation where the acceptor is in the RTIL pool and the donor is residing in between the surfactant chain of the microemulsion and the RTIL pool.

The most interesting observation is the multiple time scale of FRET and the λ_{ex} dependence. Evidently, with increase in λ_{ex} there is a marked increase in the contribution of the donor in the polar pool where FRET occurs very fast (because of short D−A distance). As is evident from Table 4, the contribution of the ultrafast FRET component (~1 ps) increases from 4% to 100% for the RTIL microemulsion and that for the water containing RTIL microemulsion increases from 12% to 100% as λ_{ex} is increased from 375 to 435 nm. It is interesting to note that at $\lambda_{ex} = 435$ nm there is no contribution of the slow FRET (in 3900 or 250 ps). This represents a situation where only the donors within the polar pool are excited. The contribution of the slow FRET component (3900 ps) decreases with increase in λ_{ex} from 375 to 435 nm for both systems.

5. Conclusion

This work shows that by varying λ_{ex} one can study FRET in different regions of an RTIL microemulsion. For the [pmim][BF_4]/TX-100/benzene microemulsion, there are three components of FRET: 1, 250, and 3900 ps in the absence of water and 1.5, 250, and 3900 ps in the presence of water. The ultrafast (1 and 1.5 ps) components of FRET are assigned to a donor and acceptor at direct contact ($R_{DA} \approx 12$ Å) in the highly polar RTIL pool of the microemulsion. The 250 ps component ($R_{DA} \approx 29$ Å) is attributed to FRET from a donor situated in between the surfactant chain and RTIL pool to an acceptor within the RTIL pool. The 3900 ps component ($R_{DA} \approx 45$ Å) may arise from FRET between a donor residing in the outer periphery of the microemulsion and an acceptor within the core of the RTIL pool and may involve diffusion of the donor outside the microemulsion into it.

Acknowledgment. Thanks are due to the Department of Science and Technology, India (Project Number: IR/I1/CF-01/2002 and J. C. Bose Fellowship) and the Council for Scientific and Industrial Research (CSIR) for generous research support. A.A., D.K.D., and D.K.S. thank CSIR for awarding fellowships.

References and Notes

(1) (a) Lei, Z.; Chen, B.; Li, C.; Liu, H. *Chem. Rev.* **2008**, *108*, 1419. (b) Castner, E. W., Jr.; Wishart, J. F.; Shirota, H. *Acc. Chem. Res.* **2007**, *40*, 1217. (c) Iwata, K.; Okajima, H.; Saha, S.; Hamaguchi, H. *Acc. Chem. Res.* **2007**, *40*, 1174. (d) Wang, Y.; Jiang, W.; Yan, T.; Voth, G. A. *Acc. Chem. Res.* **2007**, *40*, 1193. (e) Samanta, A. *J. Phys. Chem. B* **2006**, *110*, 13704. (f) Zhang, Z. C. *Adv. Catal.* **2006**, *49*, 153. (g) Rogers, R. D.; Seddon, K. R. *Science* **2003**, *302*, 792. (h) Dupont, J.; de Souza, R. F.; Suarez, P. A. Z. *Chem. Rev.* **2002**, *102*, 3667.

(2) (a) Jin, H.; Li, X.; Maroncelli, M. *J. Phys. Chem. B* **2007**, *111*, 13473. (b) Jin, H.; Baker, G. A.; Arzhantsev, S.; Dong, J.; Maroncelli, M. *J. Phys. Chem. B* **2007**, *111*, 7291. (c) Arzhantsev, S.; Jin, H.; Baker, G. A.; Maroncelli, M. *J. Phys. Chem. B* **2007**, *111*, 4978. (d) Ito, N.; Arzhantsev, S.; Heitz, M.; Maroncelli, M. *J. Phys. Chem. B* **2004**, *108*, 5771. (e) Ito, N.; Arzhantsev, S.; Maroncelli, M. *Chem. Phys. Lett.* **2004**, *396*, 83. (f) Ingram, J. A.; Moog, R. S.; Ito, N.; Biswas, R.; Maroncelli, M. *J. Phys. Chem. B* **2003**, *107*, 5926.

(3) (a) Funston, A. M.; Fadeeva, T. A.; Wishart, J. F.; Castner, E. W., Jr. *J. Phys. Chem. B* **2007**, *111*, 4963. (b) Shirota, H.; Castner, E. W., Jr. *J. Phys. Chem. A* **2005**, *109*, 9388.

(4) (a) Samanta, A. *J. Phys. Chem. B* **2006**, *110*, 13704. (b) Pal, A.; Samanta, A. *J. Phys. Chem. B* **2007**, *111*, 4724. (c) Karmakar, R.; Samanta, A. *J. Phys. Chem. A* **2002**, *106*, 6670. (d) Karmakar, R.; Samanta, A. *J. Phys. Chem. A* **2002**, *106*, 4447. (e) Paul, A.; Mandal, P. K.; Samanta, A. *J. Phys. Chem. B* **2005**, *109*, 9148. (f) Mandal, P. K.; Paul, A.; Samanta, A. *Res. Chem. Intermed.* **2005**, *31*, 575. (g) Aki, S. N. V. K.; Brennecke, J. F.; Samanta, A. *Chem. Commun.* **2001**, 413. (h) Mandal, P. K.; Sarkar, M.; Samanta, A. *J. Phys. Chem. A* **2004**, *108*, 9048. (i) Mandal, P. K.; Paul, A.; Samanta, A. *J. Photochem. Photobiol. A* **2006**, *182*, 113.

(5) (a) Triolo, A.; Russina, O.; Bleif, H.-J.; Di Cola, E. *J. Phys. Chem. B* **2007**, *111*, 4641. (b) Xiao, D.; Rajian, J. R.; Cady, A.; Li, S.; Bartsch, R. A.; Quitevis, E. L. *J. Phys. Chem. B* **2007**, *111*, 4669.

(6) (a) Kobrak, M. N. *J. Chem. Phys.* **2006**, *125*, 064502. (b) Jeong, D.; Shim, Y.; Choi, M. Y.; Kim, H. J. *J. Phys. Chem. B* **2007**, *111*, 4920. (c) Bhargava, B. L.; Balasubramanian, S. *J. Chem. Phys.* **2006**, *125*, 219901. (d) Huang, X. H.; Margulis, C. J.; Li, Y. H.; Berne, B. J. *J. Am. Chem. Soc.* **2005**, *127*, 17842. (e) Liu, X.; Zhou, G.; Zhang, S.; Wu, G.; Yu, G. *J. Phys. Chem. B* **2007**, *111*, 5658. (f) Ghatee, M. H.; Ansari, Y. *J. Chem. Phys.* **2007**, *126*, 154502. (g) Shim, Y.; Duan, J.; Choi, M. Y.; Kim, H. J. *J. Chem. Phys.* **2003**, *119*, 6441.

(7) (a) Wang, Y.; Voth, G. A. *J. Am. Chem. Soc.* **2005**, *127*, 12192. (b) Bhargava, B. L.; Devane, R.; Klein, M. L.; Balasubramanium, S. *Soft Matter* **2007**, *3*, 1395. (c) Lopes, J. N. A. C.; Padua, A. A. H. *J. Phys. Chem. B* **2006**, *110*, 3330. (d) Hu, Z.; Margulis, C. J. *Proc. Natl. Acad. Sci. U.S.A.* **2006**, *103*, 831.

(8) (a) Chowdhury, P. K.; Halder, M.; Sanders, L.; Calhoun, T.; Anderson, J. L.; Armstrong, D. W.; Petrich, J. W. *J. Phys. Chem. B* **2004**, *108*, 10245. (b) Mukherjee, P.; Crank, J. A.; Halder, M.; Armstrong, D. W.; Petrich, J. W. *J. Phys. Chem. A* **2006**, *110*, 10725. (c) Zheng, L.; Guo, C.;

Wang, J.; Liang, X.; Chen, S.; Ma, J.; Yang, B.; Jiang, Y.; Liu, H. *J. Phys. Chem. B* **2007**, *111*, 1327.

(9) (a) Seth, D.; Chakraborty, A.; Setua, P.; Sarkar, N. *J. Phys. Chem. B* **2007**, *111*, 4781. (b) Chakraborty, A.; Seth, D.; Chakrabarty, D.; Setua, P.; Sarkar, N. *J. Phys. Chem. A* **2005**, *109*, 11110. (c) Seth, D.; Chakraborty, A.; Setua, P.; Sarkar, N. *Langmuir* **2006**, *22*, 7768.

(10) (a) Eastoe, J.; Gold, S.; Rogers, S. E.; Paul, A.; Welton, T.; Heenan, R. K.; Grillo, I. *J. Am. Chem. Soc.* **2005**, *127*, 7302. (b) Gao, Y.; Li, N.; Zheng, L.; Bai, X.; Yu, L.; Zhao, X.; Zhang, J.; Zhao, M.; Li, Z. *J. Phys. Chem. B* **2007**, *111*, 2506. (c) Gao, Y.; Han, S.; Han, B.; Li, G.; Shen, D.; Li, Z.; Du, J.; Hou, W.; Zhang, G. *Langmuir* **2005**, *21*, 5681. (d) Gao, H.; Li, J.; Han, B.; Chen, W. L.; Zhang, J.; Zhang, R.; Yan, D. *Phys. Chem. Chem. Phys.* **2004**, *6*, 2914. (e) Sando, G.; Dahl, K.; Owrutsky, J. C. *J. Phys. Chem. B* **2007**, *111*, 4901. (f) Sando, G. M.; Dahl, K.; Owrutsky, J. C. *Chem. Phys. Lett.* **2006**, *418*, 402.

(11) (a) Adhikari, A.; Sahu, K.; Dey, S.; Ghosh, S.; Mandal, U.; Bhattacharyya, K. *J. Phys. Chem. B* **2007**, *111*, 12809. (b) Adhikari, A.; Dey, S.; Das, D.; Mandal, U.; Ghosh, S.; Bhattacharyya, K. *J. Phys. Chem. B* **2008**, *112*, 6350.

(12) (a) Demchenko, A. P. *Biophys. Chem.* **1982**, *15*, 101. (b) Lakowicz, J. R. *Biochemistry* **1984**, *23*, 3013. (c) Mukherjee, S.; Chattopadhyay, A. *Langmuir* **2005**, *21*, 287.

(13) (a) Satoh, T.; Okuno, H.; Tominaga, K.; Bhattacharyya, K. *Chem. Lett.* **2004**, *33*, 1090. (b) Sen, P.; Satoh, T.; Bhattacharyya, K.; Tominaga, K. *Chem. Phys. Lett.* **2005**, *411*, 339. (c) Sen, P.; Ghosh, S.; Sahu, K.; Mondal, S. K.; Bhattacharyya, K. *J. Chem. Phys.* **2006**, *124*, 204905. (d) Mandal, U.; Adhikari, A.; Dey, S.; Ghosh, S.; Mondal, S. K.; Bhattacharyya, K. *J. Phys. Chem. B* **2007**, *111*, 5896.

(14) (a) Mondal, S. K.; Ghosh, S.; Sahu, K.; Mandal, U.; Bhattacharyya, K. *J. Chem. Phys.* **2006**, *125*, 224710. (b) Ghosh, S.; Dey, S.; Adhikari, A.; Mandal, U.; Bhattacharyya, K. *J. Phys. Chem. B* **2007**, *111*, 7085. (c) Mandal, U.; Ghosh, S.; Das, D. K.; Adhikari, A.; Dey, S.; Bhattacharyya, K. *J. Chem. Sci.* **2008**, *120*, 15.

(15) (a) Namboodiri, V. V.; Varma, R. S. *Org. Lett.* **2002**, *4*, 18–3161. (b) Ding, S.; Radosz, M.; Shen, Y. *Macromolecules* **2005**, *38*, 5921. (c) Dupont, J.; Consorti, C. S.; Suarez, P. A. Z.; de Souza, R. F. *Org. Synth.* **2004**, *10*, 184.

(16) Lakowicz, J. R. *Principles of Fluorescence Spectroscopy*, 3rd ed.; Springer: New York, 2006; Chapters 9, 13, 14, and 15.

(17) Jones, G., II.; Jackson, W. R.; Choi, C.-Y.; Bergmark, W. R. *J. Phys. Chem.* **1985**, *89*, 294.

JP808777W